Supporting Information

Synthesis and Properties of the Heterospin ($S_1 = S_2 = 1/2$) Radical-Ion Salt Bis(mesitylene)molybdenum(I) [1,2,5]Thiadiazolo[3,4-c][1,2,5]thiadiazolidyl

Nikolay A. Pushkarevsky,[†,‡] Nikolay A. Semenov,[§] Alexey A. Dmitriev,[⊥,¶] Natalia V. Kuratieva,[†,‡] Artem S. Bogomyakov,[‖] Irina G. Irtegova,[§,‡] Nadezhda V. Vasilieva,[§] Bela E. Bode,[#] Nina P. Gritsan,[⊥,¶,*] Lidia S. Konstantinova,[Δ] J. Derek Woollins,[#] Oleg A. Rakitin,[Δ] Sergey N. Konchenko,[†,‡] Victor I. Ovcharenko,[‖] and Andrey V. Zibarev[§,¶,◊,*]

[†]Institute of Inorganic Chemistry, [§]Institute of Organic Chemistry, [⊥]Institute of Chemical Kinetics and Combustion and [‖]International Tomography Center, Siberian Branch of the Russian Academy of Sciences, 630090 Novosibirsk, Russia

[‡]Department of Natural Sciences and [¶]Department of Physics, Novosibirsk State University, 630090 Novosibirsk, Russia

[#]EaStCHEM School of Chemistry, University of St. Andrews, St. Andrews, Fife KY16 9ST, United Kingdom

[Δ]Institute of Organic Chemistry, Russian Academy of Sciences, 119991 Moscow, Russia

[◊]Department of Chemistry, Tomsk State University, 634050 Tomsk, Russia

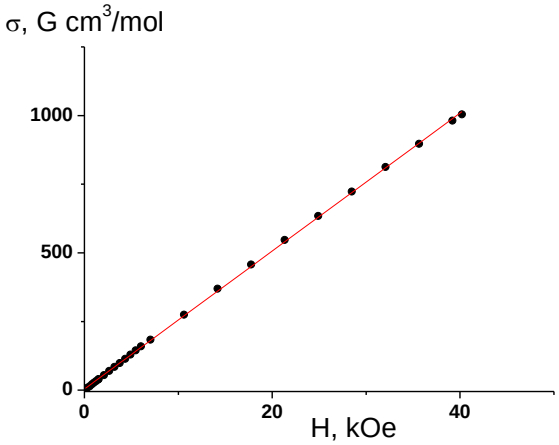

Figure S1. Field dependence of magnetization for salt **2** at 5 K. Solid line represents the linear fit $\sigma = \chi^*H + \sigma_0$ with the optimal parameters χ = 0.0251(±0.0001) cm^3 mol^{-1} and σ_0 = 4.2(±1.2) $G \cdot cm^3$ mol^{-1}. Magnetization tends to zero with a decreasing of external magnetic field strength.

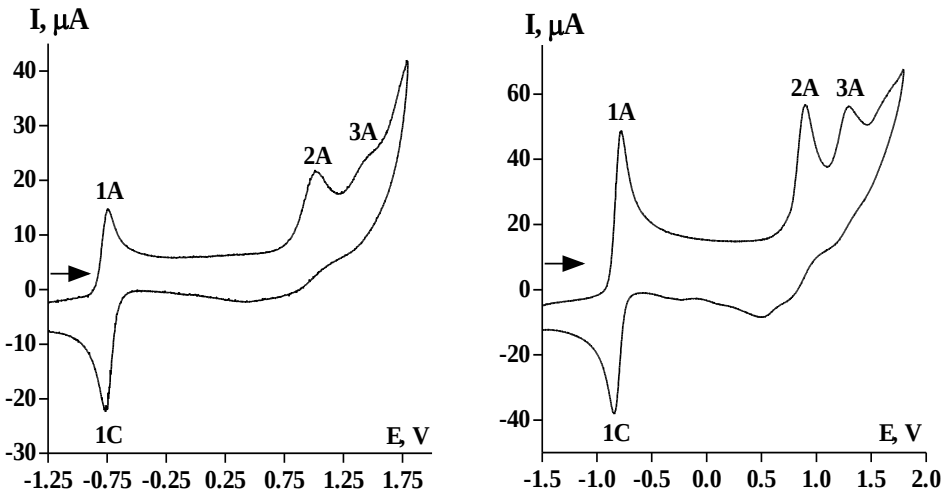

Figure S2. Cyclic voltammograms of the electrochemical oxidation of $MoTol_2$ (left) and $MoMes_2$ (right) in MeCN *vs* SCE. The beginning and direction of potential sweep are indicated by an arrow.

Table S1. Experimental peak potentials (V) derived from the electrochemical oxidation of $MoTol_2$ and $MoMes_2$ in MeCN *vs* SCE (ν = 0.1 $V \cdot s^{-1}$).

$MoAr_2$	E_p^{1A}	E_p^{2A}	E_p^{3A}	E_p^{1C}	$E_p^{1A} - E_p^{1C}$	$E_p^{1A} - E_{p/2}^{1A}$
Ar = Tol	−0.71	0.99	1.50*	−0.77	0.06	0.06
Ar = Mes	−0.79	0.92	1.32	−0.85	0.06	0.06

*Approximate value.

Variable-temperature measurements on DMF solution of salt **2** (Figure S2), as well as variable ionic strength measurements (Figure S3)[1] and quenching of RA $[\mathbf{1}]^-$ with I_2 (Figure S4), did not visualize cation $[MoMes_2]^+$ in solution EPR spectra.

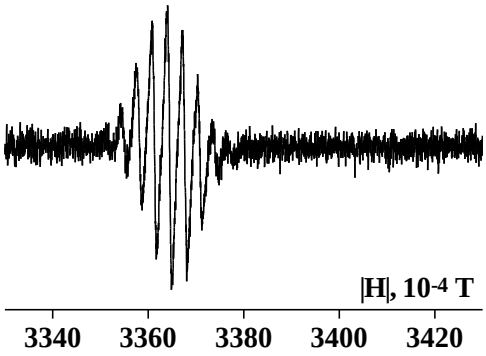

393 K

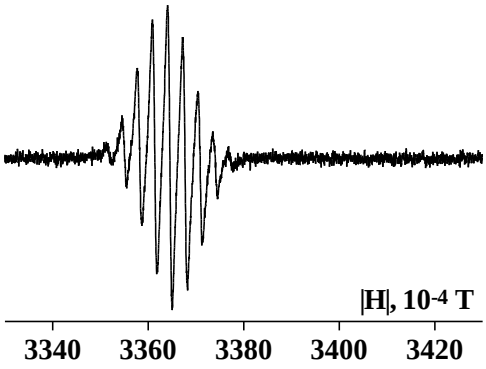

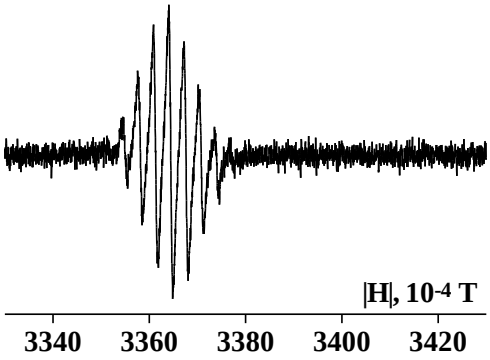

373 K

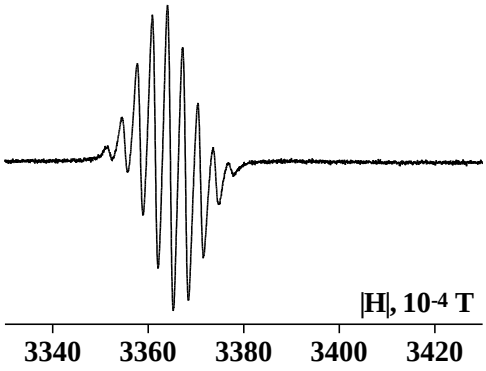

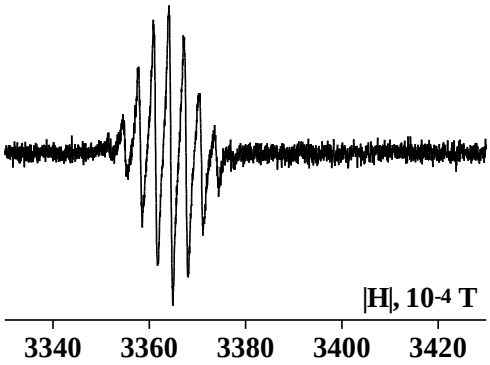

353 K

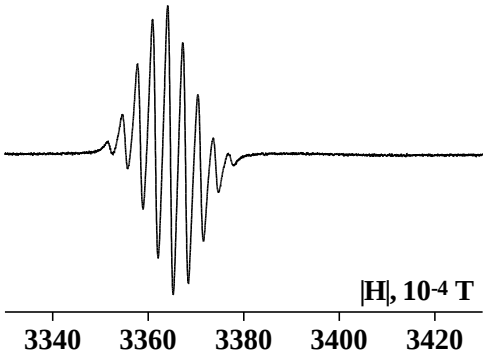

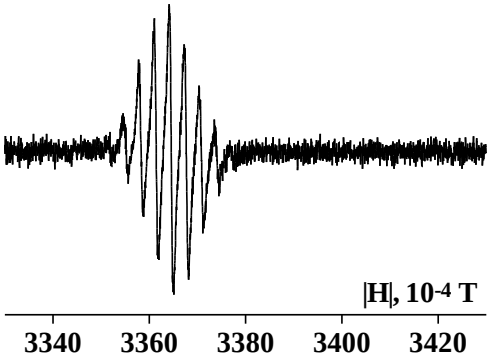

333 K

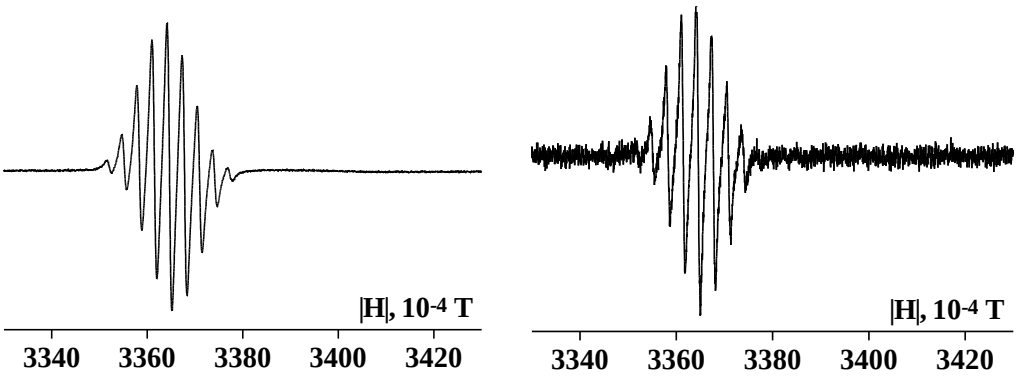

313 K

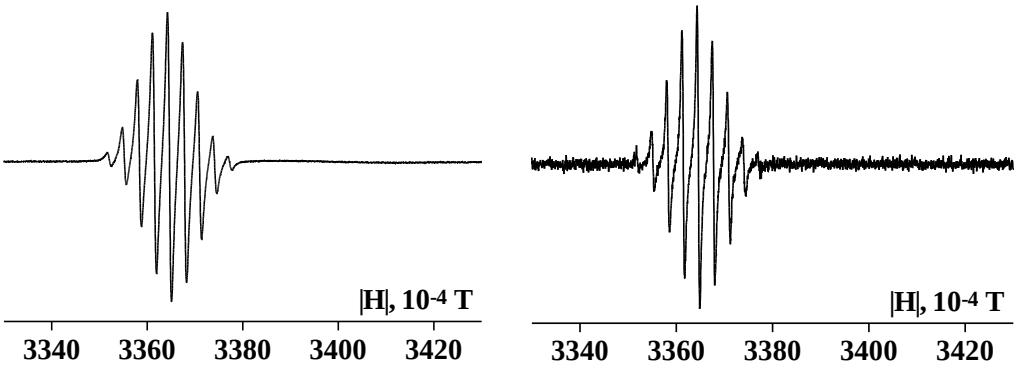

293 K

283 K

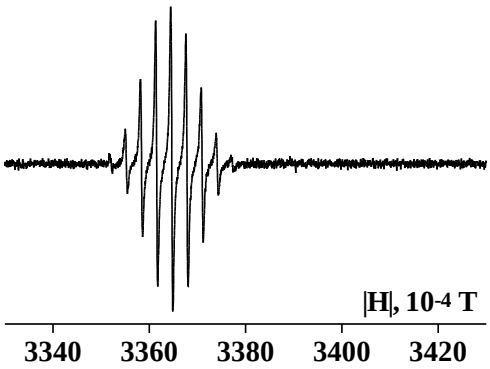

260 K

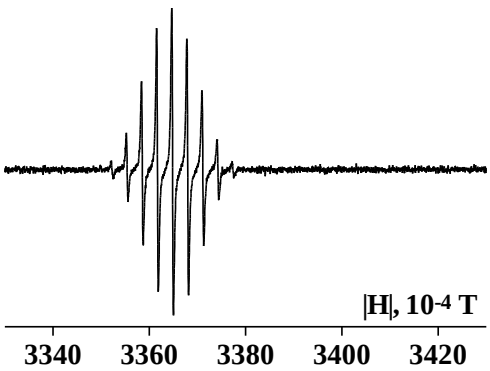

240 K

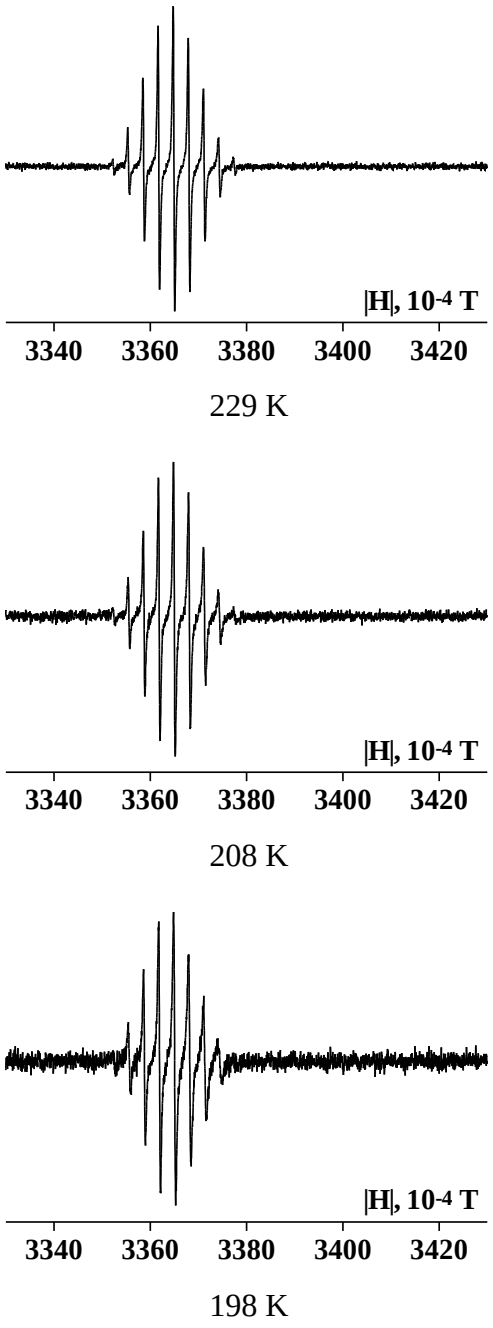

Figure S3. EPR spectra of salt **2** in DMF solution from independent measurements in temperature range 198−393 K with experimental temperature going up (left) and down (right). At 393 K decomposition of **2** begins.

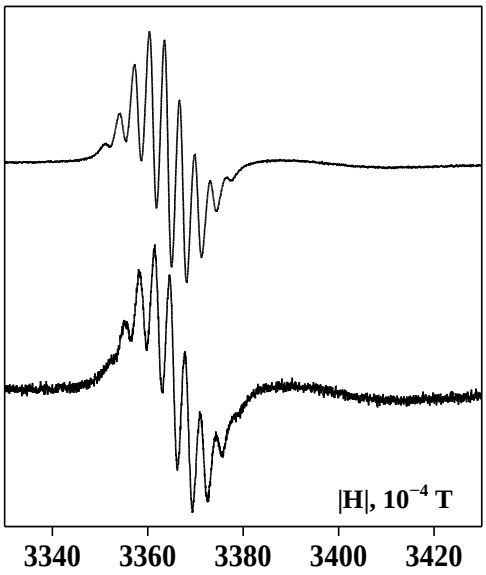

Figure S4. EPR spectra of salt **2** at 295 K: in DMF (above) and in 0.1 M solution of Bu_4NBF_4 in DMF (below).

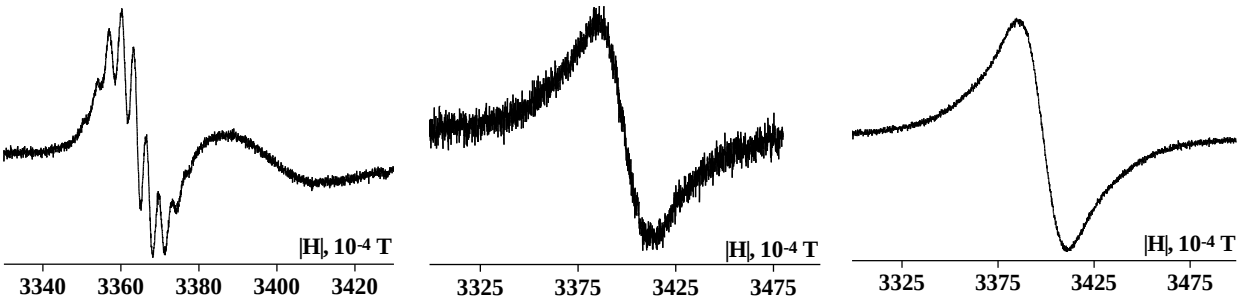

Figure S5. EPR spectra of DMF solution of salt **2** before (left) and after (middle) adding I_2 The EPR spectrum of $MoMes_2 + I_2$ system in DMF, g = 1.9852 (right).

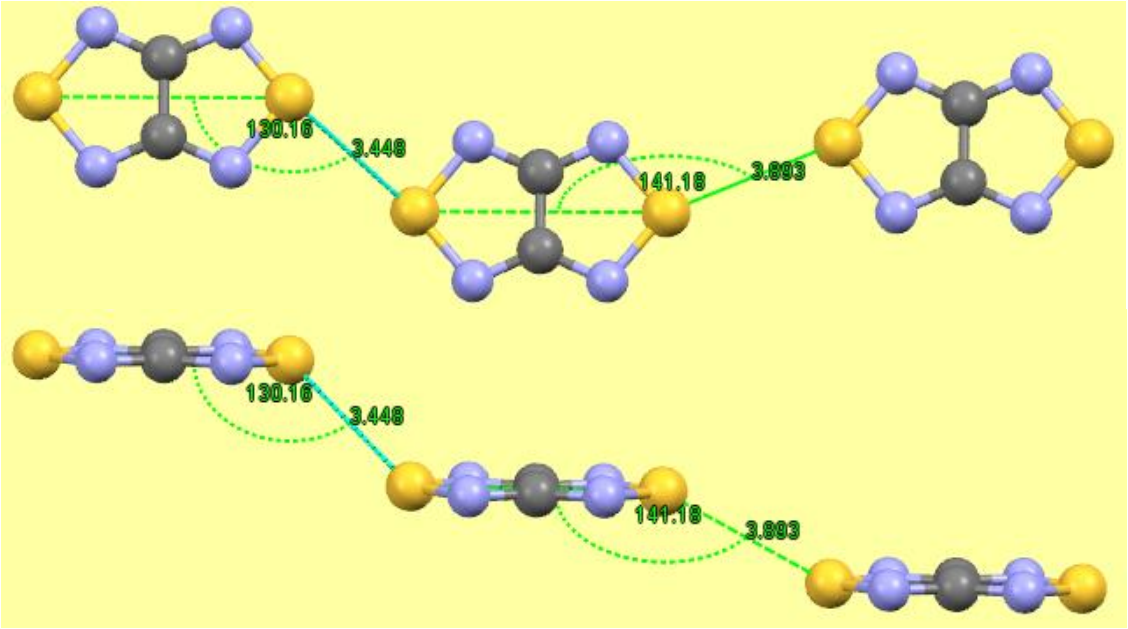

Figure S6. Two views of the alternating magnetic chain of RAs $[\mathbf{1}]^{-}$ in the XRD structure of salt **2**.

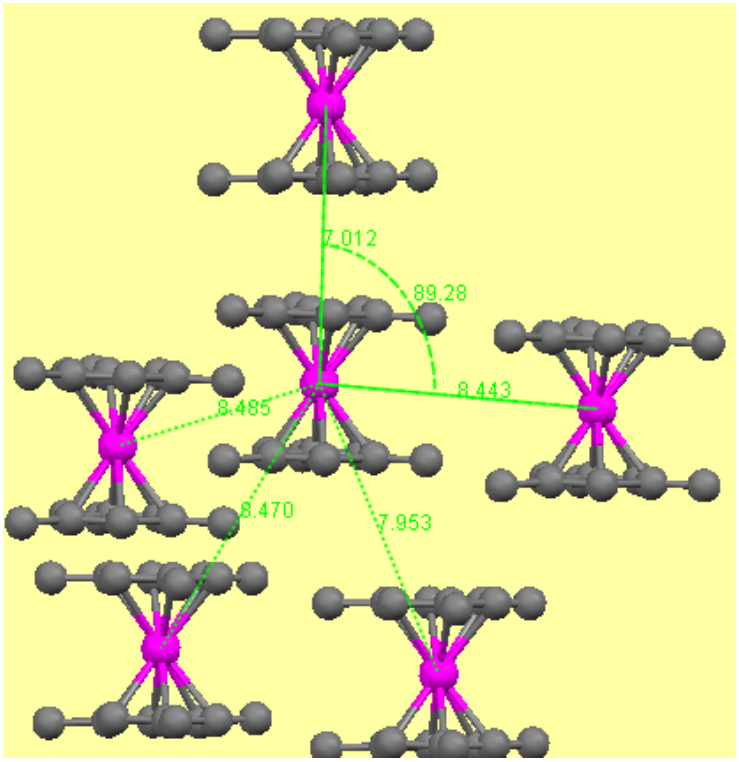

Figure S7. Fragment of the XRD structure of salt **2** featuring spatial arrangement of nearest-neighboring cations $[MoMes_2]^{+}$.

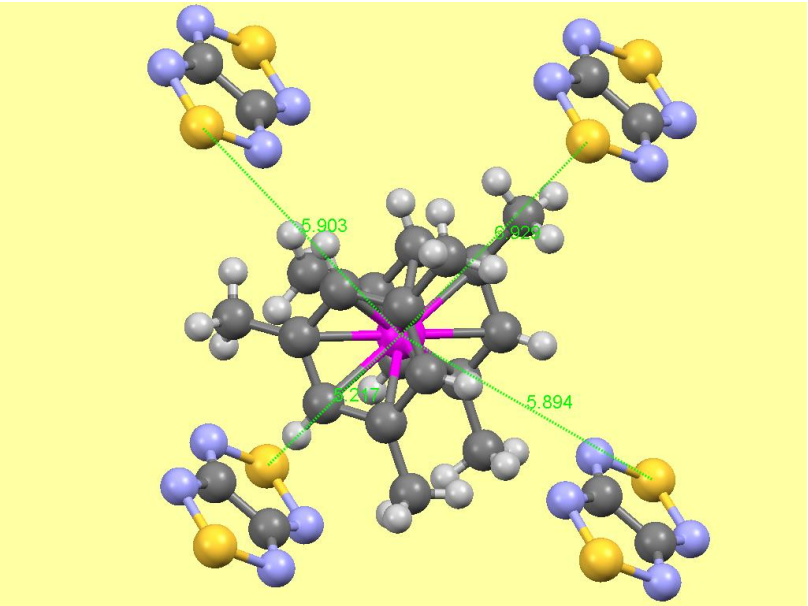

Figure S8. Spatial arrangement of RAs $[\mathbf{1}]^-$ around the cation $[MoMes_2]^+$ in the XRD structure of salt **2**.

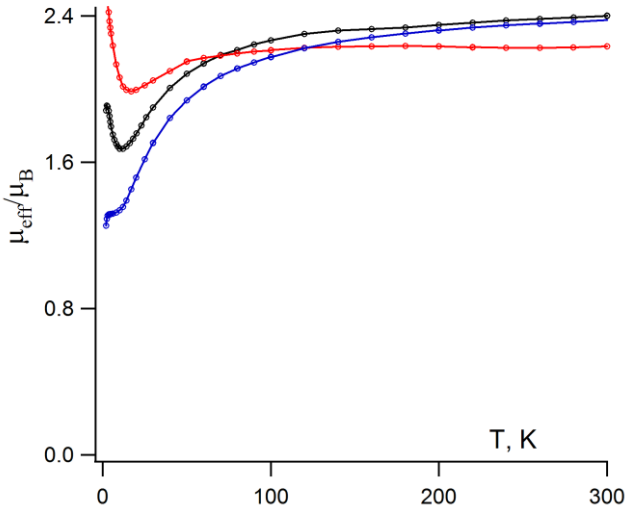

Figure S9. Magnetic properties of partially decomposed samples of salt **2**, time span from blue to red. It is seen that progressive decomposition leads to low-temperature growth of the effective magnetic moment.

Single-crystal XRD data for $[Cp^*CrS]_4$ (Figure S9) were collected at 150(2) K with a Bruker Nonius X8 Apex diffractometer equipped with a 4K CCD area detector, with graphite-monochromated Mo Kα radiation (λ = 0.71073 Å). The standard φ- and φ/ω-scan techniques

were employed to measure intensities. Absorption corrections were applied using the SADABS program.[2] The crystal structures were solved by direct methods and refined by full-matrix least-squares method with the SHELXTL software package.[2] All non-hydrogen atoms were refined anisotropically. Hydrogen atoms of organic ligands were placed in the calculated positions and refined as riding on their parent C atoms. Complete crystallographic data have been deposited at the Cambridge Crystallographic Data Center (ref. number CCDC 1053125) and may be obtained free of charge from the CCDC, 12 Union Road, Cambridge, CB2 1 EZ, UK (fax: +44-1223-336033; http://www.ccdc.cam.ac.uk/conts/retrieving.html).

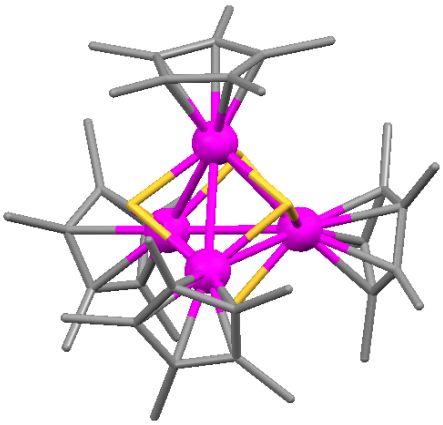

Figure S10. XRD structure of pentamethylcyclopentadienyl-capped cubane cluster Cr_4S_4 obtained from reduction of [1,2,5]thiadiazolo[3,4-b]quinoxaline with decamethylchromocene.

For discussion of structure and bonding in such type cubane clusters, see ref. 3.

References and Notes

(1) It is known that RA salts of 1,2,5-chalcogenadiazoles and related heterocycles exist in solution in the form of contact ion-pairs: (a) Bagryanskaya, I. Yu.; Gatilov, Yu. V.; Gritsan, N. P.; Ikorskii, V. N.; Irtegova, I. G.; Lonchakov, A. V.; Lork, E.; Mews, R.; Ovcharenko, V. I.; Semenov, N. A.; Vasilieva, N. V.; Zibarev, A. V. *Eur. J. Inorg. Chem.* **2007**, *2007*, 4751–4761. (b) Bock, H.; Haenel, P.; Neidlein, R. *Phosphorus Sulfur* **1988**, *39*, 235–252. (c) Kaim, W. *J. Organomet. Chem.* **1984**, *264*, 317–326. (d) Hanson, P. *Adv. Heterocycl. Chem.* **1980**, *27*, 31–149. (e) Gerson, F.; Plattner, G.; Bartetzko, R.; Gleiter, R. *Helv. Chim. Acta* **1980**, *63*, 2144–

2151. (f) Kwan, C. L.; Carmack, M.; Kochi, J. K. *J. Phys. Chem.* **1976**, *80*, 1786–1792. (g) Kamiya, M.; Akahori, Y. *Bull. Chem. Soc. Jpn.* **1970**, *43*, 268–271. (h) Fajer, J.; Bielski, B. H. J.; Felton, R. H. *J. Phys. Chem.* **1968**, *72*, 1281–1288. (i) Atherton, N. M.; Ockwell, J. N.; Dietz, R. *J. Chem. Soc. A* **1967**, 771–777. (j) Strom, E. T.; Russell, G. A. *J. Am. Chem. Soc.* **1965**, *87*, 3326–3329.

(2) (a) *APEX2* (version 1.08), *SAINT* (version 7.03) and *SADABS* (version 2.11), Bruker AXS Inc. (b) *SHELXTL* (version 6.12), Bruker Advanced X-Ray Solutions: Madison, WI, USA, 2004.

(3) (a) McGrady, J. E. *J. Chem. Soc*., *Dalton Trans*. **1999**, 1393–1399. (b) Song, L.-C.; Cheng, H.-W.; Chen, X.; Hu, Q.-M. *Eur. J. Inorg. Chem.* **2004**, *2004*, 3147–3153.